

Nanoparticle–Graphene based Nanocomposites

Subjects: Nanoscience & Nanotechnology

Contributor: Ana Maria Diez-Pascual

Bacterial infections are a leading cause of death in both Europe and USA. The use of antibacterial nanomaterials is a very promising approach to combat the microorganisms due to their high specific surface area and intrinsic or chemically incorporated antibacterial action. Graphene, a two dimensional carbon nanomaterial with excellent mechanical, thermal, and electrical properties, and its derivatives, like graphene oxide (GO) and reduced graphene oxide (rGO), are very good candidates for controlling microbial infections. Nonetheless, the mechanisms of antimicrobial action, their cytotoxicity, and other issues continue imprecise. This review offers select examples on the leading advances in the development of antimicrobial nanocomposites incorporating inorganic nanoparticles and graphene or its derivatives, with the goal of providing a improved understanding of the antibacterial properties of graphene-based nanomaterials.

Keywords: antibacterial activity ; nanocomposites ; bacterial infection ; antibiotic resistance ; graphene ; graphene oxide ; reduced graphene oxide

1. Introduction

While graphene-based materials exhibit antibacterial properties, they have a strong tendency to agglomerate, in particular G and rGO, due to strong van der Waals interactions among the sheets, which condition their antibacterial action. This issue can be prevented via formation of nanocomposites by surface modification with metal ions/oxides NPs. Inorganic NPs can enhance graphene properties due to their high surface area-to-volume ratio, which leads to novel chemical, electrical, mechanical, optical, and electro-optical properties that differ from those of their bulk counterparts. Further, the mixing of G and rGO with metal oxide NPs can improve their dispersibility in polar solvents such as water^[1]. Thus, numerous nanocomposites have been developed over recent years that combine the bactericide action of inorganic nanoparticles with the inherent antibacterial property of graphene-based nanomaterials to attain synergistic effects, and the most representative examples will be reviewed in the following sections.

2. Nanocomposites with Silver Nanoparticles

The antibacterial properties of Ag⁺ and Ag-based composites have been comprehensively explored^[2]. Ag⁺ can damage the bacterial membranes and also produce ROS via photocatalytic activation. Nonetheless, when Ag nanoparticles interact with bacteria, they agglomerate; hence their effective specific surface area decreases, leading to reduced antibacterial action^[3]. To solve this issue, nanocomposites of graphene and Ag nanoparticles were developed^{[4][5]}, although the improvements in antibacterial activity were still limited. Therefore, numerous studies have been reported on GO and rGO nanocomposites comprising Ag nanoparticles^{[6][7][8][9][10][11][12][13][14][15][16][17]}(Table 1), showing improved performance compared to GO and Ag nanoparticles alone due to synergistic effects; further, the mixture of both constituents considerably reduces the concentrations required to inhibit all bacteria. Thus, significantly higher antibacterial activity was found for AgNPs-GO composites (1:2 ratio), with an average NP size of 80 nm^[7] at a concentration of 200 µg/mL (Table 1), compared to that of GO or AgNPs, attributed to a higher ROS production, hence resulting in stronger oxidative stress and disruption of the cell membrane. Further, the AgNPs attached to GO are more stable and well-dispersed, which also contributes to the higher efficacy. Comparable antibacterial action has been found for similar composites with smaller nanoparticles (ca. 40 nm) for an optimal AgNPs:GO ratio of 1:1 even at concentrations as low as 2.5 µg/mL^[13].

Table 1. Antibacterial properties of nanocomposites with graphene-based materials and inorganic NPs (S: spherical; QS: quasi-spherical; E: ellipsoidal; C: cubic; T: triangular; NW: nanowire; ST: star).

Graphene Material	NP shape/size (Φ, nm)	Bacteria Model	Concentration (µg/mL)	Inhibition (%)	Ref.
AgNPs-GO	S/93	<i>S. enteritidis</i>	200	61	[6]

Graphene Material	NP shape/ size (Φ , nm)	Bacteria Model	Concentration ($\mu\text{g/mL}$)	Inhibition (%)	Ref.
AgNPs-GO	S/80	<i>E. coli</i>	200	89	[7]
AgNPs-GO	S/80	<i>S. epidermidis</i>	200	76	[7]
AgNPs-GO	S/80	<i>S. aureus</i>	200	81	[7]
AgNPs-GO	S/80	<i>C. albicans</i>	200	78	[7]
AgNPs-GO	S, QS	<i>E. coli/S. aureus</i>	100	100	[8]
AgNPs-GO	QSI40	<i>E. coli</i>	6.4	100	[10]
AgNPs-GO	QSI60	<i>E. coli/S. aureus</i>	10	100	[11]
AgNPs-GO	E/98	<i>E. coli/S. aureus</i>	45	100	[12]
AgNPs-GO	S/40	<i>E. coli</i>	2.5	80	[13]
AgNPs-GO	S/40	<i>S. aureus</i>	2.5	78	[13]
AgNPs-GO	S/3.1	<i>S. aureus</i>	64	100	[17]
AgNPs-GO	S/3.1	<i>C. albicans</i>	64	100	[17]
AgNPs-GO	S/3.1	<i>E. coli/P. aeruginosa</i>	128	100	[17]
AgNPs-rGO	QSI57	<i>E. coli</i>	40	100	[9]
AgNPs-rGO	S/12	<i>E. coli</i>	20	100	[14]
Au-rGO	T, S/50	<i>S. aureus/B. subtilis</i>	250	94	[18]
Au-rGO	T, S/50	<i>E. coli/P. aeruginosa</i>	250	50	[18]
Au-rGO	T, S	<i>E. coli</i>	10	99	[19]
Cu ₂ ONPs-rGO	C/30	<i>E. coli</i>	40	70	[20]
Cu ₂ ONPs-rGO	C/30	<i>S. aureus</i>	40	65	[20]
CuONPs-GO	E/80	<i>E. coli</i>	3.0	90	[21]
CuONPs-GO	E/80	<i>S. typhimurium</i>	3.0	99	[21]
TiO ₂ -GO	S/30	<i>E. coli</i>	180	100	[22]
ZnO-GO	NW/75	<i>E. coli</i>	500	100	[23]
ZnO-GO	ST/150	<i>E. coli/P. aeruginosa</i>	6.5	100	[24]
ZnO-GO	ST/150	<i>S. aureus</i>	11.5	100	[24]
ZnO-GO	ST/150	<i>B. subtilis</i>	15.0	100	[24]
ZnO-G	S/20	<i>E. coli</i>	3.0	100	[25]
Ag-Fe ₂ O ₃ -rGO	QS	<i>E. coli</i>	0.1	100	[26]
Fe ₂ O ₃ -GO	S/225	<i>E. coli</i>	100	97	[27]
MnFe ₂ O ₄ -GO	S/170	<i>E. coli</i>	100	82	[28]
Ag-CoFe ₂ O ₄ -rGO	QSI75	<i>E. coli/S. aureus</i>	12	98	[29]
Fe ₃ O ₄ -GO	S/66	<i>E. coli</i>	300	91	[30]

Bacterial cell disruption seems to be the main mechanism against Gram-negative bacteria, while the inhibition of cell division could account for the lysis of Gram-positive ones. AgNPs-GO nanocomposites cause stronger damage towards *E. coli* membrane compared to *S. aureus*, as can be observed in Table 1. Thus, the antimicrobial potential of these nanocomposites is also influenced by the thickness of the cell wall of the microorganisms. The wall of Gram-positive contains a thick layer (20–80 nm) of peptidoglycan attached to teichoic acids. In Gram-negative bacteria, the cell wall comprises of a thin (7–8 nm) peptidoglycan layer and an outer membrane. The thicker peptidoglycan layer in Gram-

positive bacteria could account for their higher resistance towards the effects of AgNPs-GO. Their bactericide action can be depicted in four stages (Figure 1)^[15]: release of Ag⁺ ions, penetration through the cell membrane, ROS generation, followed by DNA, protein, mitochondrion, lipids and membrane damage, which finally leads to cell death.

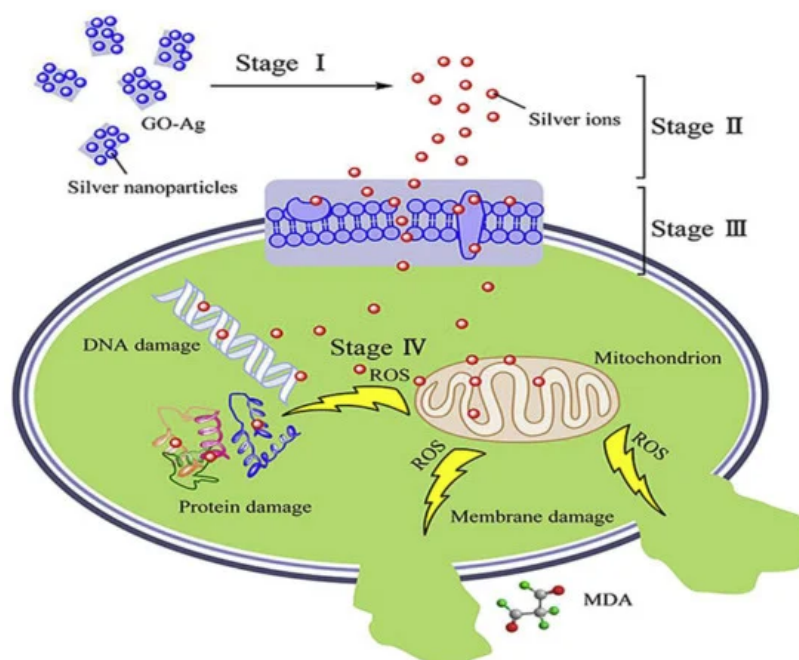


Figure 1. Representation of the antimicrobial action of AgNP-GO nanocomposites. Reproduced from Ref.^[15], with permission from Elsevier, 2016.

Lipids constitute a main target during oxidative stress. Free radicals can directly attack the polyunsaturated fatty acids in the bacteria, yeast their membranes, and activate peroxidation of lipids, resulting in a drop in membrane fluidity, which can significantly disrupt membrane-bound proteins. DNA is also a key target. Mechanisms of DNA damage include abstractions and addition reactions by free radicals, leading to carbon-centered sugar radicals and OH- or H-adduct radicals of heterocyclic bases. The sugar moieties creating single- and double-strand breaks in the backbone, adducts of base and sugar groups, and cross-links to other molecules can block replication^[31].

It is worthy to mention that AgNPs-rGO nanocomposites as antibacterial agents are more limited due to the tendency of the nanosheets to aggregate via strong van der Waals interactions. While the interaction between G (or rGO) and Ag⁺ should be mainly via hydrophobic and van der Waals forces, Ag⁺ nanoparticles have been reported to interact with the negatively charged oxygen-containing functional groups on the GO surface via electrostatic binding^[10]. The AgNP-GO nanocomposites showed improved colloidal stability, photo-stability, and antibacterial activities against Gram-negative bacteria compared to AgNPs alone. GO plays a key role in improving the stability of the AgNPs, acting as a platform to prevent their agglomeration. Moreover, composites comprising smaller AgNPs showed better antibacterial activity than those with bigger NPs. This effect of the nanoparticle size has been further corroborated by different authors. Thus, the antibacterial efficacy of AgNP-GO with four NP sizes (10, 30, 50, and 80 nm) against *E. coli* and *S. aureus* has been tested, and it was found that the composite with the smallest NP showed the best activity^[16]. Similarly, a recent study^[17] investigated the bactericide action of AgNP-GO (ratio 1:2.3) manufactured via an environmentally friendly one-step approach, which comprised of spherical NPs with different diameters. The smallest NPs (ca. 3.1 nm) were obtained for the lowest concentrations of the silver precursor and the lowest synthesis temperatures, and led to an exceptional antibacterial action against Gram-negative *E. coli* and *P. aeruginosa*, as well as Gram-positive *S. aureus* and *C. albicans* (Table 1). Small-sized AgNPs have a larger surface area, resulting in more efficient cell-particle contact.

3. Nanocomposites with Gold Nanoparticles

The antibacterial activity of gold NPs also depends on their size and shape. Those of smaller dimensions (ca. less than 2 nm) are more likely to penetrate the bacterial cells and cause cell damage, followed by death^[32]. Further, triangular-shaped NPs display better activity towards Gram-positive and Gram-negative bacteria than spherical ones^[33], since their sharp edges can pierce the membranes of endosomes and translocate to the cytoplasm where they can be retained. The NPs can anchor to the bacterial membrane by electrostatic interaction and disrupt its integrity. They can alter the membrane potential and reduce the ATP levels within the cell, inhibiting the binding of tRNA with ribosomal subunit and thus disturbing translation^[34]. Further, Au NPs can produce holes in the cell wall causing leakage of cell contents, and

bind with the DNA, hindering transcription. They are also able to generate oxidative via free radical formation: the interaction between small NPs and bacteria probably induces a metabolic imbalance in the bacterial cell, resulting in an increase of ROS production that concluded in bacteria death^[32].

Au nanoparticles have also been integrated with GO and rGO^{[18][19]}. These composites also possess higher antibacterial activity than the individual components, and the bacterial cell disruption seems to be induced by the leak of sugars and proteins from the cell membrane when it comes in contact with the nanocomposite^[18]. Further, Au nanostructures wrapped by rGO modified with polyethylene glycol (PEG) have been recently applied for the photothermal ablation of bacteria^[19], and optimal inhibition of *E. coli* was attained at high temperatures (56–70 °C), Figure 2. This novel biocompatible process for pathogen ablation opens up a new perspective for treatment of urinary infections.

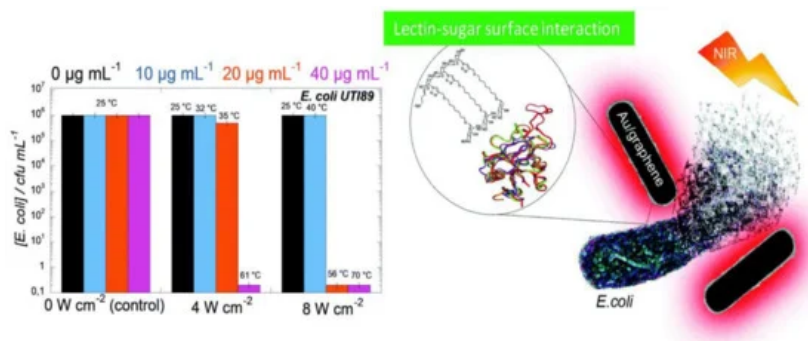


Figure 2. *E. coli* viability in the presence of rGO–PEG–Au NPs upon irradiation at 4 or 8 W cm⁻² for 10 min. Reproduced from Ref. ^[19], with permission from the Royal Society of Chemistry, 2015.

4. Nanocomposites with Cooper Oxide Nanoparticles

A few studies have also been devoted to investigating the antibacterial action of Cu^[35], Cu₂O^{[36][20]} or CuO^[21] nanoparticles bound to GO or rGO. At high concentrations, these nanomaterials are toxic to the majority of microorganisms since the redox properties of Cu provoke cellular damage including protein and lipid oxidation. Thus, it is crucial to control the release of Cu²⁺ ions, which produce ROS species on the bacterial surface. Cu₂O can interact with GO and rGO nanosheets via physisorption, electrostatic attraction, or charge-transfer. The nanocomposites have improved bactericidal properties than each individual component, since the graphenic nanosheets can stimulate the Cu₂O to generate more ROS^[20], and also prevent nanosheet aggregation. Simultaneously, rGO prevents Cu₂O from reacting with the environment and releasing Cu²⁺ rapidly.

In a recent study^[20], the antibacterial properties of Cu₂O nanoparticles and a rGO-Cu₂O nanocomposite were compared as a function of time (Figure 3a,b). When the samples were stored in phosphate buffered saline (PBS) for less than seven days, the nanocomposite showed about 14% higher antibacterial activity against *E. coli* and *S. aureus* than the Cu₂O nanoparticles, which only produced ROS until the third day, while the nanocomposite systematically produced ROS during this period. For longer periods, the activity of the nanocomposite was considerably higher than that of Cu₂O (i.e., 40% and 35% better against *E. coli* and *S. Aureus* after one month). The antibacterial mechanism seems to be based on ROS generation (Figure 3d). Upon light illumination, the photoinduced electron would be transferred from the Cu₂O to the rGO, which could suppress the recombination of electron-hole pairs. The rGO could accept the photoexcited electrons from Cu₂O, enabling improved charge transfer between the bacteria and the rGO-Cu₂O nanocomposite^[36].

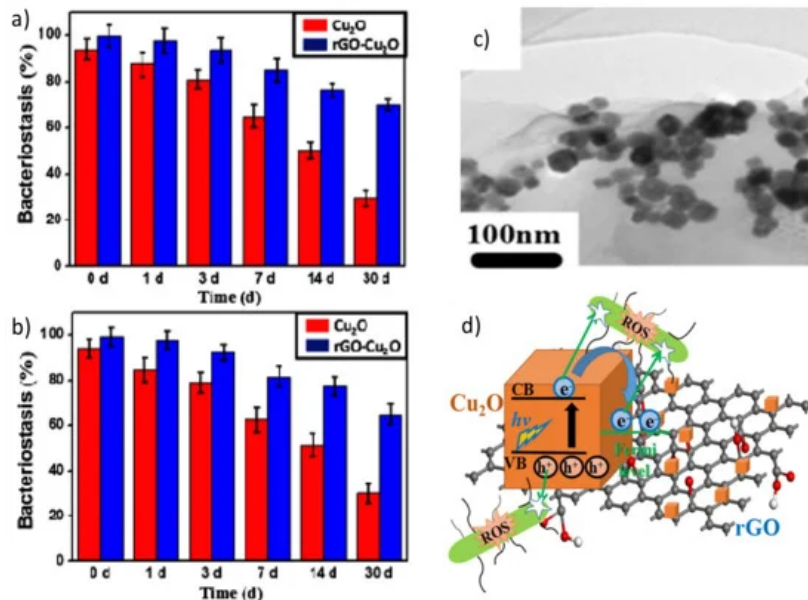


Figure 3. Percentage of bacterial reduction of *E. coli* (a) and *S. aureus* (b) in the presence of Cu_2O nanoparticles and the Cu_2O -rGO nanocomposite after immersion in phosphate buffered saline (PBS) for different days. TEM image of the Cu_2O -rGO nanocomposite (c). Schematic representation of the mechanism of ROS production of the Cu_2O -rGO nanocomposite (d). Reproduced from Ref. [20], with permission from Elsevier, 2019.

Nanocomposites of CuO nanoparticles and GO have also been developed [21], which were found to be effective antibacterial nanomaterials, strongly inhibiting the proliferation of both *E. coli* and *S. typhimurium* bacteria compared to GO or CuO alone. The surface morphology of the nanocomposite significantly differed from that of the pure components (Figure 4), as revealed by scanning electron microscopy (SEM), transmission electron microscopy (TEM), and atomic force microscopy (AFM), and this could account for the improved bactericide action. An inspection of the nanomaterial surface (Figure 4c,e) shows the underlying sheets of GO covered by a high concentration of well-dispersed ellipsoidal NPs, with the short and long axis dimensions being ~80 nm and ~190 nm, respectively. AFM imaging (Figure 4f,g) revealed that the GO and GO-CuO flakes were about 12 and 13 nm in thickness, respectively, indicating that the nanocomposite is composed of a few layers of GO covered by a thin CuO coating. The energy-dispersive X-ray (EDX) mapping confirmed that the material on the modified GO contains copper and oxygen.

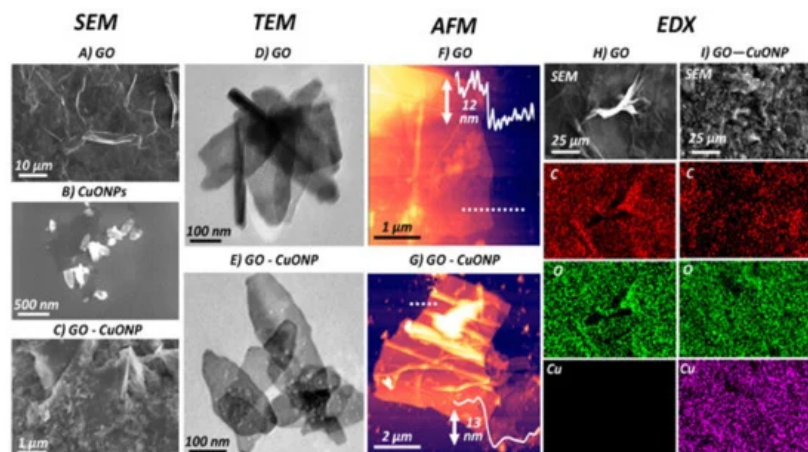


Figure 4. SEM images of (A) GO, (B) CuO nanoparticles, and (C) GO-CuO nanocomposite. (D and E) TEM and (F and G) AFM images of GO and GO-CuO, respectively. Energy-dispersive X-ray (EDX) spectral map for H) GO and I) GO-CuO nanocomposite. Reprinted from Ref. [21], with permission from the American Chemical Society, 2019.

5. Nanocomposites with Titanium Oxide Nanoparticles

TiO_2 is an important semiconducting material due to its chemical inertness, non-toxicity, low cost, excellent chemical/thermal stability, high UV absorption, and strong antibacterial activity against a large variety of microorganisms [37][38][39]. A few works have been recently reported on the photocatalytic antibacterial properties of GO and rGO nanocomposites incorporating TiO_2 [40][41][42], which provide a green and effective method for the inactivation of various microorganisms by generating ROS. The photocatalytic activity of TiO_2 improves after coupling with G derivatives, attributed to the remarkable electron conductivity of the carbon nanomaterial that provides a 2D network reservoir to

accept as well as shuttle photogenerated electrons from the semiconductor, which results in the separation and prolonged lifetime of hole-electron pairs^[43]. Further, GO can interact with TiO₂ via H-bonding and polar forces, while in the case of rGO, the hydrophobic interactions play a dominant role. The antibacterial activity of a GO-TiO₂ nanocomposites against *E. coli*. was investigated, and a complete inactivation was found under light irradiation for 30 min at a concentration of 180 µg/mL^[22], Table 1. The inexpensiveness of TiO₂ and the easiness of manufacturing magnetic GO-TiO₂ make them suitable for water disinfection treatment. In addition, cotton fabrics have been covered with rGO decorated with TiO₂ nanoparticles in order to provide self-cleaning characteristics and improve the antimicrobial properties^[44], and the nanocomposite coating strongly restricted the growth of *E. faecalis* and *S. aureus*. In general, studies indicate higher activity of rGO-TiO₂ against Gram-positive bacteria compared to Gram-negative ones. rGO-TiO₂ nanocomposites have also been developed for the synergetic degradation of fluoroquinolone in a pulse discharge plasma (PDP) system^[42], and the highest removal efficiency (99.4%) was attained at 5 wt% rGO content, which was 23.7% higher than that for TiO₂ alone.

6. Nanocomposites with Zinc Oxide Nanoparticles

ZnO is another semiconductor photocatalyst widely used as an antibacterial agent^{[44][45]}. Its properties depend mainly on its specific surface area and the number of surface sites at which reactions take place with absorbed molecules. The release of Zn²⁺ has been proposed as one of the principal antibacterial mechanisms of these nanoparticles, together with the penetration and disruption of the bacterial membrane^[46]. Nonetheless, as occurs with other nanoparticles, agglomeration hinders efficient antibacterial action. The mixing of GO or rGO with ZnO nanoparticles can prevent their aggregation, leading to nanocomposites with good environmental stability and better antibacterial properties than each of the components alone^{[47][48][49][50][51][52][53][54]}. ZnO-GO nanoparticles have been prepared via a simple one pot reaction^[50] in which the GO aided the ZnO dispersion, slowed down the ZnO dissolution and acted as an anchorage point, favoring the direct intimate contact bacteria-ZnO.

The mechanism of photocatalytic inactivation of *E. coli* by GO-ZnO nanocomposites has also been investigated^[51], and it was reported that GO promoted the charge transfer, favoring the bulk production of ROS, hence improving the bacterial inactivation efficiency. ZnO/graphene quantum dot nanocomposites have been synthesized via the hydrothermal method^[53] and showed enhanced antibacterial activity on *E. coli* compared to the individual components, attributed to superior ROS production under UV-irradiation. Further, ZnO nanoparticles on GO^[54] were able to inhibit the growth of *E. coli*, *S. typhimurium*, *B. subtilis*, and *E. faecalis* bacteria (Figure 5), after 24 h of incubation. Excellent antibacterial activity of the nanocomposite can be observed with minimum inhibitory concentrations (MIC) of 6.25 µg/mL for *E. coli* and *S. typhimurium*, 12.5 µg/mL for *B. subtilis*, and 25 µg/mL for *E. faecalis*, significantly lower than those found for the individual components. This proves that GO-ZnO nanocomposites at low concentration can be effectively used to inhibit the growth of bacteria.

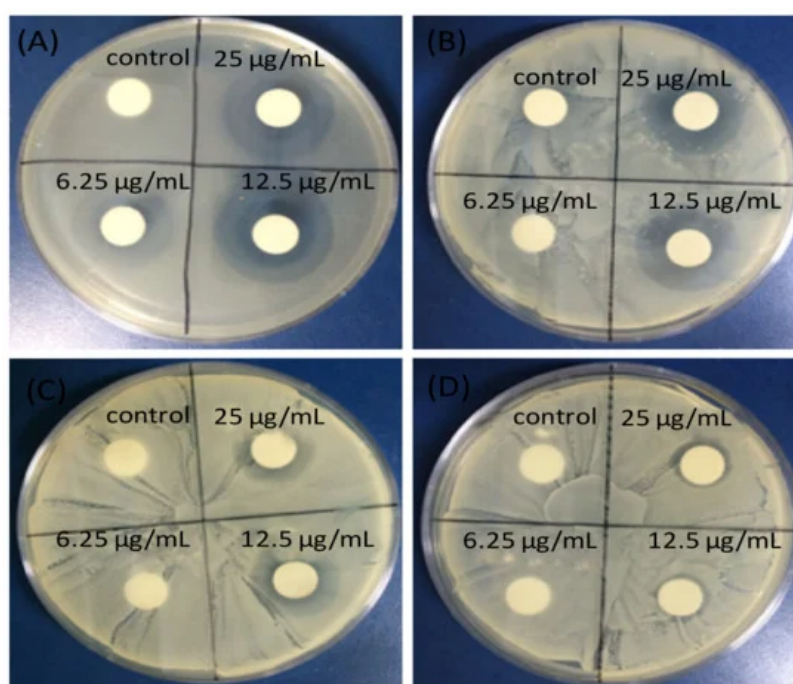


Figure 5. Inhibitory zones of ZnO-GO nanocomposite against (A) *Escherichia coli*; (B) *Salmonella typhimurium*; (C) *Bacillus subtilis*; (D) *Enterococcus faecalis*. Adapted from Ref.^[54], with permission from Dove Medical Press, 2015.

This enhanced behaviour is ascribed to cell membrane disruption due to the release of the Zn^{2+} ions and the ROS production. Thus, Zn^{2+} can link to the negatively charged bacterial membrane, causing the protein on the membrane to solidify, thus inhibiting the bacterial proliferation. Besides, electrons can be quickly transferred between the ZnO nanoparticles and the GO, and subsequently absorb surface oxygen to form ROS, resulting in the formation of lipid peroxide, consequently damaging the bacterial membrane.

The nanocomposite synthesis method also influences the antibacterial activity. Those prepared via electrophoretic deposition (EPD) showed better properties than those manufactured via drop-casting^[47]. Thus, the EPD method led to effective penetration of the negatively charged GO sheets into ZnO nanowires to form a spider net-like structure, whereas the drop-casting technique caused only the surface coverage of the GO sheets onto the nanowires. The ZnO nanowires alone could just inactivate 58% of *E. coli*, while both drop-casting and EPD-prepared GO/ZnO nanocomposites displayed significant antibacterial activity; in particular, the EPD one caused 99.5% photoinactivation under visible light irradiation for 1 h at a concentration of 500 $\mu\text{g}/\text{mL}$, Table 1.

7. Multicomponent Nanocomposites

Several graphene-based multicomponent composites have been prepared by incorporating different nanoparticles with graphene or its derivatives, in order to attain improved antibacterial activity due to synergistic effects. For instance, GO-Ag-TiO₂ nanocomposite coatings were synthesized using a hydrothermal process for the control of the food-borne pathogen *Campylobacter jejuni*. The nanocomposites efficiently inhibited the aggregation and growth of *C. jejuni* as well as biofilm formation^[55]. Different nanocomposites incorporating iron oxide nanoparticles have also been developed^{[26][27][28][29][30]}, Table 1. Magnetic GO-MnFe₂O₄ hybrids at a concentration of 100 $\mu\text{g}/\text{mL}$ led to about 82% inhibition on *E. coli* after only 2 h of contact^[28]. Hybrids with polyethylenimine wrapped Ag nanoparticles and Fe₂O₃ caused 100% inhibition of *E. coli* at a concentration of only 0.1 $\mu\text{g}/\text{mL}$ ^[26]. A multicomposite of GO, CoFe₂O₄, and Ag nanoparticles was also manufactured to disinfect water contaminated with *E. coli* and *S. aureus*, leading to almost complete inhibition at 12 $\mu\text{g}/\text{mL}$ ^[29]. GO decorated with Ag, TiO₂, and ZnO nanostructures has been prepared via ultrasonication and casting, and the antibacterial activity of the nanocomposite was tested against Gram-positive *S. aureus* and *B. anthracoides* and Gram-negative *E. coli* and *P. multocida*^[56]. Figure 6 shows SEM images of GO, Ag, GO-Ag, GO-TiO₂-ZnO, and GO-Ag-TiO₂-ZnO nanocomposites.

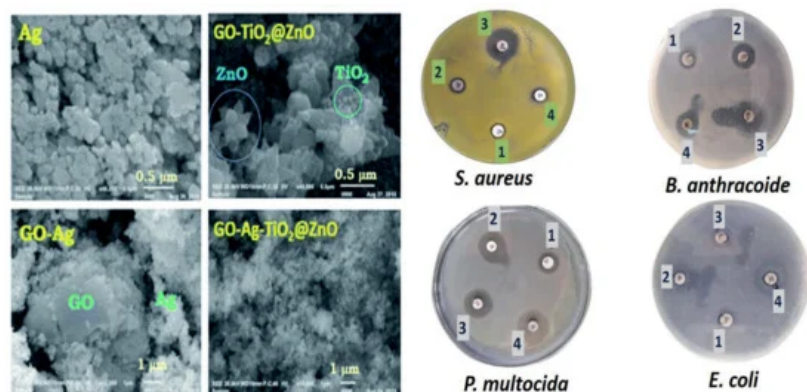


Figure 6. Left: SEM images of Ag, GO-Ag, GO-TiO₂@ZnO, and GO-Ag-TiO₂@ZnO nanocomposite. Right: Inhibitory zones of GO-Ag-TiO₂@ZnO nanocomposite against *S. aureus*, *B. anthracoides* and Gram-negative *E. coli* and *P. multocida*. Adapted from Ref. ^[56], with permission from the Royal Society of Chemistry, 2019.

As can be observed, the GO nanosheet was densely packed by the metal oxides, representative of a good combination between the carbon nanomaterial and the inorganic NPs. Thus, the GO nanosheets seem to act as bridges for the metal oxide NPs. Ag NPs have a spherical morphology and are located on the GO surface. The ZnO nanoflower appears over the GO surface, while the spherical TiO₂ is deposited onto the ZnO nanoflower. The Ag NPs alone had the lowest inhibitory effect on all tested bacteria. The GO-TiO₂-ZnO nanocomposite showed highly suppressing microbial growth against both Gram-positive and Gram-negative bacteria, while the four-component nanocomposite was found to be the most effective against Gram-negative bacteria (Figure 10). The improved activity of the hybrid was ascribed to the synergistic effect of the different components: direct damage of the cellular membrane by the Ag nanoparticles, ROS generation by the TiO₂ and ZnO, contact between the GO sharp edges and the bacteria, and the accumulation of the nanoparticles in the cytoplasm.

Ag/ZnO/rGO nanocomposites with different weight ratios were synthesized via rapid microwave irradiation^[57]. Depending on the composition, the hybrids were more effective against Gram positive or Gram negative bacteria, and the optimal performance was found at 7 wt% Ag and 15 wt% ZnO. Further, multifunctional nanocomposites of GO incorporating both Ag and Fe₂O₃ nanoparticles were prepared and characterized^[58]. The MIC values against *E. coli* and *S. aureus* were 0.025 and 0.05 mg/mL, respectively. These composites display both antibacterial and magnetic properties, and can be harvested with a magnet.

On the other hand, hydroxyapatite (HA) (Ca₁₀(PO₄)₆(OH)₂), has excellent biocompatibility, osteoconductivity, is non-toxic, and is widely used for biomedical applications^[59]. rGO/HA/Ag multicomponent nanocomposites have been prepared using the hydrothermal method^[60] and characterized via different spectroscopic techniques. They showed improved antibacterial activity against *B. cereus*, *S. aureus*, *E. coli* and *K. pneumonia* than the pure components.

Overall, the comparison of the data in Table 1 reveals that the optimum bactericide efficacy at the lowest concentration (0.1 µg/mL) is attained for the hybrid nanocomposite comprising Ag⁺ NPs, rGO and Fe₃O₄, with an antibacterial performance superior to those ever reported for photothermal materials, arising from the synergistic effect of the three components^[26].

References

1. Andrew T. Smith; Anna Marie Lachance; Songshan Zeng; Bin Liu; Luyi Sun; Synthesis, properties, and applications of graphene oxide/reduced graphene oxide and their nanocomposites. *Nano Materials Science* **2019**, *1*, 31-47, [10.1016/j.nanoms.2019.02.004](#).
2. Loris Rizzello; Pier Paolo Pompa; Nanosilver-based antibacterial drugs and devices: Mechanisms, methodological drawbacks, and guidelines. *Chemical Society Reviews* **2014**, *43*, 1501-1518, [10.1039/c3cs60218d](#).
3. Aleš Panáček; Libor Kvítek; Robert Prucek; Milan Kolář; Renata Večeřová; Naděžda Pizúrová; Virender K. Sharma; Tatjana Nevěčná; Radek Zbořil; Silver Colloid Nanoparticles: Synthesis, Characterization, and Their Antibacterial Activity. *The Journal of Physical Chemistry B* **2006**, *110*, 16248-16253, [10.1021/jp063826h](#).
4. Tong, Y.; Bohm, S.; Song, M.; Graphene based materials and their composites as coatings. *Austin. J. Nanomed. Nanotechnol.* **2004**, *1*, 1003, .
5. Zengjie Fan; Bin Liu; Jinqing Wang; Songying Zhang; Qianqian Lin; Peiwei Gong; Limin Ma; Shengrong Yang; A Novel Wound Dressing Based on Ag/Graphene Polymer Hydrogel: Effectively Kill Bacteria and Accelerate Wound Healing. *Advanced Functional Materials* **2014**, *24*, 3933-3943, [10.1002/adfm.201304202](#).
6. Wierzbicki, M.; Jaworski, S.; Sawosz, E.; Jung, A.; Gielerak, G.; Jaremek, H.; Łojkowski, W.; Woźniak, B.; Stobiński, L.; Małolepszy, A.; et al. Graphene oxide in a composite with silver nanoparticles reduces the fibroblast and endothelial cell cytotoxicity of an antibacterial nanoplatform. *Nanoscale Res. Lett.* **2019**, *14*, 320.
7. Jaworski, S.; Wierzbicki, M.; Sawosz, E.; Jung, A.; Gielerak, G.; Biernat, J.; Jaremek, H.; Łojkowski, W.; Woźniak, B.; Wojnarowicz, J.; et al. Graphene oxide-based nanocomposites decorated with silver nanoparticles as an antibacterial agent. *Nanoscale Res. Lett.* **2018**, *13*, 116.
8. Nguyen, V.H.; Kim, B.-K.; Jo, Y.-L.; Shim, J.-J. Preparation and antibacterial activity of silver nanoparticles-decorated graphene composites. *J. Supercrit. Fluids* **2012**, *72*, 28–35.
9. Moghayed, M.; Goharshadi, E.K.; Ghazvini, K.; Ahmadzadeh, H.; Ranjbaran, L.; Masoudi, R.; Ludwig, R. Kinetics and mechanism of antibacterial activity and cytotoxicity of Ag-RGO nanocomposite. *Coll. Surf. B Biointerfaces* **2017**, *159*, 366–374.
10. Zhu, Z.; Su, M.; Ma, L.; Ma, L.; Liu, D.; Wang, Z. Preparation of graphene oxide–silver nanoparticle nanohybrids with highly antibacterial capability. *Talanta* **2013**, *117*, 449–455.
11. Ganguly, S.; Das, P.; Bose, M.; Das, T.K.; Mondal, S.; Das, A.K.; Das, N.C. Sonochemical green reduction to prepare Ag nanoparticles decorated graphene sheets for catalytic performance and antibacterial application. *Ultrasonics Sonochem.* **2017**, *39*, 577–588.
12. Bao, Q.; Zhang, D.; Qi, P. Synthesis and characterization of silver nanoparticle and graphene oxide nanosheet composites as a bactericidal agent for water disinfection. *J. Colloid Interface Sci.* **2011**, *360*, 463–470.
13. Tang, J.; Chen, Q.; Xu, L.Q.; Zhang, S.; Feng, L.; Cheng, L.; Xu, H.; Liu, Z.; Peng, R. Graphene oxide–silver nanocomposite as a highly effective antibacterial agent with species-specific mechanisms. *ACS Appl. Mater. Interfaces* **2013**, *5*, 3867–3874.
14. Zhou, Y.; Yang, J.; He, T.; Shi, H.; Cheng, X.; Lu, Y. Highly stable and dispersive silver nanoparticle–graphene composites by a simple and low-energy-consuming approach and their antimicrobial activity. *Small* **2013**, *9*, 3445–3454.

15. Song, B.; Zhang, C.; Zeng, G.; Gong, J.; Chang, Y.; Jiang, Y. Antibacterial properties and mechanism of graphene oxide-silver nanocomposites as bactericidal agents for water disinfection. *Arch. Biochem. Biophys.* 2016, 604, 167–176.
16. Chen, X.; Huang, X.; Zheng, C.; Liu, Y.L.; Xu, T.; Liu, J. Preparation of different sized nano-silver loaded on functionalized graphene oxide with highly effective antibacterial properties. *J. Mater. Chem. B* 2015, 3, 7020.
17. Cobos, M.; de-la-Pinta, I.; Quindós, G.; Fernández, M.J.; Fernández, M.A. Graphene oxide–silver nanoparticle nanohybrids: Synthesis, characterization, and antimicrobial properties. *Nanomaterials* 2020, 10, 376.
18. Najrul Hussain; Animesh Gogoi; Rupak K. Sarma; Ponchami Sharma; Alexandre Barras; Rabah Boukherroub; Ratul Saikia; Pinaki Sengupta; Manash R. Das; Reduced Graphene Oxide Nanosheets Decorated with Au Nanoparticles as an Effective Bactericide: Investigation of Biocompatibility and Leakage of Sugars and Proteins. *ChemPlusChem* **2014**, 79, 1774-1784, [10.1002/cplu.201402240](https://doi.org/10.1002/cplu.201402240).
19. Kostiantyn Turcheniuk; Charles Henri Hage; Jolanda Spadavecchia; Aritz Yanguas Serrano; Iban Larroulet; Amaia Pesquera; Amaia Zurutuza; Mariano Gonzalez Pisfil; Laurent Heliot; Julie Boukaert; et al. Plasmonic photothermal destruction of uropathogenic E. coli with reduced graphene oxide and core/shell nanocomposites of gold nanorods/reduced graphene oxide.. *Journal of Materials Chemistry B* **2014**, 3, 375-386, [10.1039/c4tb01760a](https://doi.org/10.1039/c4tb01760a).
20. Zhaoqing Yang; Xiangping Hao; Shougang Chen; Zhenqing Ma; Wenhui Wang; Caiyu Wang; Longfei Yue; Haiyun Sun; Qian Shao; Vignesh Murugadoss; et al. Long-term antibacterial stable reduced graphene oxide nanocomposites loaded with cuprous oxide nanoparticles.. *Journal of Colloid and Interface Science* **2018**, 533, 13-23, [10.1016/j.jcis.2018.08.053](https://doi.org/10.1016/j.jcis.2018.08.053).
21. Piumie Rajapaksha; Samuel Cheeseman; Stuart Hombusch; Billy James Murdoch; Sheeana Gangadoo; Ewan W. Blanche; Yen Truong; Daniel Cozzolino; Chris F. McConville; Russell J. Crawford; et al. Antibacterial Properties of Graphene Oxide–Copper Oxide Nanoparticle Nanocomposites. *ACS Applied Bio Materials* **2019**, 2, 5687-5696, [10.1021/acsabm.9b00754](https://doi.org/10.1021/acsabm.9b00754).
22. Ying-Na Chang; Xiao-Ming Ou; Guang-Ming Zeng; Jilai Gong; Can-Hui Deng; Yan Jiang; Jie Liang; Gang-Qiang Yuan; Hong-Yu Liu; Xun He; et al. Synthesis of magnetic graphene oxide–TiO₂ and their antibacterial properties under solar irradiation. *Applied Surface Science* **2015**, 343, 1-10, [10.1016/j.apsusc.2015.03.082](https://doi.org/10.1016/j.apsusc.2015.03.082).
23. Amin Nourmohammadi; Reza Rahighi; Omid Akhavan; Alireza Moshfegh; Graphene oxide sheets involved in vertically aligned zinc oxide nanowires for visible light photoinactivation of bacteria. *Journal of Alloys and Compounds* **2014**, 612, 380-385, [10.1016/j.jallcom.2014.05.195](https://doi.org/10.1016/j.jallcom.2014.05.195).
24. S. Archana; K. Yogesh Kumar; B.K. Jayanna; Sharon Olivera; A. Anand; M.K. Prashanth; Handanahally Basavarajiah Muralidhara; Versatile Graphene oxide decorated by star shaped Zinc oxide nanocomposites with superior adsorption capacity and antimicrobial activity. *Journal of Science: Advanced Materials and Devices* **2018**, 3, 167-174, [10.1016/j.jsamd.2018.02.002](https://doi.org/10.1016/j.jsamd.2018.02.002).
25. Dan Wu; Taicheng An; Guiying Li; Wei Wang; Yuncheng Cai; Ho Yin Yip; Huijun Zhao; Po Keung Wong; Mechanistic study of the visible-light-driven photocatalytic inactivation of bacteria by graphene oxide–zinc oxide composite. *Applied Surface Science* **2015**, 358, 137-145, [10.1016/j.apsusc.2015.08.033](https://doi.org/10.1016/j.apsusc.2015.08.033).
26. Ning Wang; Bo Hu; Ming-Li Chen; Jian-Hua Wang; Polyethylenimine mediated silver nanoparticle-decorated magnetic graphene as a promising photothermal antibacterial agent. *Nanotechnology* **2015**, 26, 195703, [10.1088/0957-4484/26/19/195703](https://doi.org/10.1088/0957-4484/26/19/195703).
27. Chella Santhosh; Pratap Kollu; Sejal Doshi; Madhulika Sharma; Dharendra Bahadur; Mudaliar T. Vanchinathan; P. Saravanan; Byeong-Su Kim; Andrews Nirmala Grace; Adsorption, photodegradation and antibacterial study of graphene–Fe₃O₄ nanocomposite for multipurpose water purification application. *RSC Advances* **2014**, 4, 28300-28308, [10.1039/c4ra02913e](https://doi.org/10.1039/c4ra02913e).
28. Santhosh Chella; Pratap Kollu; EswaraVara Prasadarao Komarala; Sejal Doshi; Murugan Saranya; Sathiyathan Felix; Rajendran Ramachandran; Padmanapan Saravanan; Vijaya Lakshmi Koneru; Velmurugan Venugopal; et al. Solvothermal synthesis of MnFe₂O₄-graphene composite—Investigation of its adsorption and antimicrobial properties. *Applied Surface Science* **2015**, 327, 27-36, [10.1016/j.apsusc.2014.11.096](https://doi.org/10.1016/j.apsusc.2014.11.096).
29. Shuanglong Ma; Sihui Zhan; Yanan Jia; Qixing Zhou; Highly Efficient Antibacterial and Pb(II) Removal Effects of Ag-Co Fe₂O₄-GO Nanocomposite. *ACS Applied Materials & Interfaces* **2015**, 7, 10576-10586, [10.1021/acsami.5b02209](https://doi.org/10.1021/acsami.5b02209).
30. Can-Hui Deng; Jilai Gong; Guang-Ming Zeng; Cheng-Gang Niu; Qiu-Ya Niu; Wei Zhang; Hong-Yu Liu; Inactivation performance and mechanism of Escherichia coli in aqueous system exposed to iron oxide loaded graphene nanocomposites. *Journal of Hazardous Materials* **2014**, 276, 66-76, [10.1016/j.jhazmat.2014.05.011](https://doi.org/10.1016/j.jhazmat.2014.05.011).
31. Mahmuda Akter; Tajuddin Sikder; Mostafizur Rahman; A.K.M. Atique Ullah; Kaniz Fatima Binte Hossain; Subrata Banik; Toshiyuki Hosokawa; Takeshi Saito; Masaaki Kurasaki; A systematic review on silver nanoparticles-induced cytotoxicity

- y: Physicochemical properties and perspectives.. *Journal of Advanced Research* **2017**, 9, 1-16, [10.1016/j.jare.2017.10.008](https://doi.org/10.1016/j.jare.2017.10.008).
32. M.R. Bindhu; M. Umadevi; Antibacterial activities of green synthesized gold nanoparticles. *Materials Letters* **2014**, 120, 122-125, [10.1016/j.matlet.2014.01.108](https://doi.org/10.1016/j.matlet.2014.01.108).
33. S.L. Smitha; K.G. Gopchandran; K.G. Gopchandran; Surface enhanced Raman scattering, antibacterial and antifungal active triangular gold nanoparticles. *Spectrochimica Acta Part A: Molecular and Biomolecular Spectroscopy* **2013**, 102, 114-119, [10.1016/j.saa.2012.09.055](https://doi.org/10.1016/j.saa.2012.09.055).
34. Akhilesh Rai; Asmita Prabhune; Carole Celia Perry; Antibiotic mediated synthesis of gold nanoparticles with potent anti microbial activity and their application in antimicrobial coatings. *Journal of Materials Chemistry* **2010**, 20, 6789, [10.1039/c0jm00817f](https://doi.org/10.1039/c0jm00817f).
35. Yu Ouyang; Xiang Cai; Qingshan Shi; Lili Liu; Dongliang Wan; Shaozao Tan; You-Sheng Ouyang; Poly-L-lysine-modified reduced graphene oxide stabilizes the copper nanoparticles with higher water-solubility and long-term additively antibacterial activity. *Colloids and Surfaces B: Biointerfaces* **2013**, 107, 107-114, [10.1016/j.colsurfb.2013.01.073](https://doi.org/10.1016/j.colsurfb.2013.01.073).
36. Mingyan Wang; JunRao Huang; Zhiwei Tong; Weihua Li; Jun Chen; Reduced graphene oxide–cuprous oxide composite via facial deposition for photocatalytic dye-degradation. *Journal of Alloys and Compounds* **2013**, 568, 26-35, [10.1016/j.jallcom.2013.03.019](https://doi.org/10.1016/j.jallcom.2013.03.019).
37. Ana M. Díez-Pascual; Angel L. Díez-Vicente; Nano-TiO₂ Reinforced PEEK/PEI Blends as Biomaterials for Load-Bearing Implant Applications. *ACS Applied Materials & Interfaces* **2015**, 7, 5561-5573, [10.1021/acsami.5b00210](https://doi.org/10.1021/acsami.5b00210).
38. Ana Maria Diez Pascual; Angel L. Díez-Vicente; Development of linseed oil-TiO₂ green nanocomposites as antimicrobial coatings.. *Journal of Materials Chemistry B* **2015**, 3, 4458-4471, [10.1039/c5tb00209e](https://doi.org/10.1039/c5tb00209e).
39. Ana Maria Diez Pascual; Angel L. Díez-Vicente; Effect of TiO₂ nanoparticles on the performance of polyphenylsulfone biomaterial for orthopaedic implants.. *Journal of Materials Chemistry B* **2014**, 2, 7502-7514, [10.1039/c4tb01101e](https://doi.org/10.1039/c4tb01101e).
40. Jincheng Liu; Lei Liu; Hongwei Bai; Yinjie Wang; Darren Delai Sun; Gram-scale production of graphene oxide–TiO₂ nanorod composites: Towards high-activity photocatalytic materials. *Applied Catalysis B: Environmental* **2011**, 106, 76–82, [10.1016/j.apcatb.2011.05.007](https://doi.org/10.1016/j.apcatb.2011.05.007).
41. Miruna Stan; Ionela C Nica; Marcela Popa; Mariana C Chifiriuc; Ovidiu Iordache; Iuliana Dumitrescu; Lucian Diamandescu; Anca Dinischiotu; Reduced graphene oxide/TiO₂ nanocomposites coating of cotton fabrics with antibacterial and self-cleaning properties. *Journal of Industrial Textiles* **2018**, 49, 277-293, [10.1177/1528083718779447](https://doi.org/10.1177/1528083718779447).
42. He Guo; Nan Jiang; Huijuan Wang; Kefeng Shang; Na Lu; Jie Li; Yan Wu; Enhanced catalytic performance of graphene-TiO₂ nanocomposites for synergetic degradation of fluoroquinolone antibiotic in pulsed discharge plasma system. *Applied Catalysis B: Environmental* **2019**, 248, 552-566, [10.1016/j.apcatb.2019.01.052](https://doi.org/10.1016/j.apcatb.2019.01.052).
43. Selim Arif Sher Shah; A Reum Park; Kan Zhang; Jong Hyeok Park; Pil J. Yoo; Green Synthesis of Biphasic TiO₂–Reduced Graphene Oxide Nanocomposites with Highly Enhanced Photocatalytic Activity. *ACS Applied Materials & Interfaces* **2012**, 4, 3893-3901, [10.1021/am301287m](https://doi.org/10.1021/am301287m).
44. Ana M. Díez-Pascual; Angel L. Díez-Vicente; High-Performance Aminated Poly(phenylene sulfide)/ZnO Nanocomposites for Medical Applications. *ACS Applied Materials & Interfaces* **2014**, 6, 10132-10145, [10.1021/am501610p](https://doi.org/10.1021/am501610p).
45. Ana M. Díez-Pascual; Angel L. Díez-Vicente; Epoxidized Soybean Oil/ZnO Biocomposites for Soft Tissue Applications: Preparation and Characterization. *ACS Applied Materials & Interfaces* **2014**, 6, 17277-17288, [10.1021/am505385n](https://doi.org/10.1021/am505385n).
46. Ana M. Díez-Pascual; Angel L. Díez-Vicente; Development of Nanocomposites Reinforced with Carboxylated Poly(ether ether ketone) Grafted to Zinc Oxide with Superior Antibacterial Properties. *ACS Applied Materials & Interfaces* **2014**, 6, 3729-3741, [10.1021/am500171x](https://doi.org/10.1021/am500171x).
47. Nourmohammadi, A.; Rahighi, R.; Akhavan, O.; Moshfegh, A. Graphene oxide sheets involved in vertically aligned zinc oxide nanowires for visible light photoinactivation of bacteria. *J. Alloys Comp.* 2014, 612, 380–385.
48. Trinh, L.T.; Quynh, L.A.B.; Hieu, N.H. Synthesis of zinc oxide/graphene oxide nanocomposite material for antibacterial application. *Int. J. Nanotechnol.* 2018, 15, 108–117.
49. Archana, S.; Kumar, K.Y.; Jayanna, B.; Olivera, S.; Anand, A.; Prashanth, M.; Muralidhara, H. Versatile Graphene oxide decorated by star shaped Zinc oxide nanocomposites with superior adsorption capacity and antimicrobial activity. *J. Sci. Adv. Mater. Devices* 2018, 3, 167–174.
50. Wang, Y.-W.; Cao, A.; Jiang, Y.; Zhang, X.; Liu, J.-H.; Liu, Y.; Wang, H. Superior antibacterial activity of zinc oxide/graphene oxide composites originating from high zinc concentration localized around bacteria. *ACS Appl. Mater. Interfaces* 2014, 6, 2791–2798.

51. Wu, D.; An, T.; Li, G.; Wang, W.; Cai, Y.; Yip, H.Y.; Zhao, H.; Wong, P.K. Mechanistic study of the visible-light-driven photocatalytic inactivation of bacteria by graphene oxide–zinc oxide composite. *Appl. Surf. Sci.* 2015, 358, 137–145.
52. Kavitha, T.; Gopalan, A.I.; Lee, K.-P.; Park, S.-Y. Glucose sensing, photocatalytic and antibacterial properties of graphene–ZnO nanoparticle hybrids. *Carbon* 2012, 50, 2994–3000.
53. Liu, J.; Rojas-Andrade, M.D.; Chata, G.; Peng, Y.; Roseman, G.; Lu, J.-E.; Millhauser, G.L.; Saltikov, C.; Chen, S. Photo-enhanced antibacterial activity of ZnO/graphene quantum dot nanocomposites. *Nanoscale* 2018, 10, 158–166.
54. Zhong, L.; Yun, K. Graphene oxide-modified ZnO particles: Synthesis, characterization, and antibacterial properties. *Int. J. Nanomed.* 2015, 10, 79–92.
55. Zobia Noreen; N.R. Khalid; Rashda Abbasi; Sundus Javed; Imran Ahmad; Habib Bokhari; Visible light sensitive Ag/TiO₂/graphene composite as a potential coating material for control of *Campylobacter jejuni*. *Materials Science and Engineering: C* **2018**, 98, 125-133, [10.1016/j.msec.2018.12.087](https://doi.org/10.1016/j.msec.2018.12.087).
56. Nagi El-Shafai; Mohamed E. El-Khouly; Maged El-Kemary; Mohamed E. El-Khouly; Ibrahim Eldesoukey; Mamdouh Ma soud; Graphene oxide decorated with zinc oxide nanoflower, silver and titanium dioxide nanoparticles: fabrication, characterization, DNA interaction, and antibacterial activity. *RSC Advances* **2019**, 9, 3704-3714, [10.1039/c8ra09788g](https://doi.org/10.1039/c8ra09788g).
57. Yi-Huang Hsueh; Chien-Te Hsieh; Shu-Ting Chiu; Ping-Han Tsai; Chia-Ying Liu; Wan-Ju Ke; Chiu; Tsai; Liu; Ke; et al. Antibacterial Property of Composites of Reduced Graphene Oxide with Nano-Silver and Zinc Oxide Nanoparticles Synthesized Using a Microwave-Assisted Approach. *International Journal of Molecular Sciences* **2019**, 20, 5394, [10.3390/ijms20215394](https://doi.org/10.3390/ijms20215394).
58. Raziieh Moosavi; Sahana Ramanathan; Yeong Yuh Lee; Karen Chong Siew Ling; Abbas Afkhami; Govindaraju Archuna n; Parasuraman Padmanabhan; Balázs Gulyás; Mitali Kakran; Subramanian Tamil Selvan; et al. Synthesis of antibacterial and magnetic nanocomposites by decorating graphene oxide surface with metal nanoparticles. *RSC Advances* **2015**, 5, 76442-76450, [10.1039/c5ra15578a](https://doi.org/10.1039/c5ra15578a).
59. Ana Maria Diez Pascual; Angel L. Díez-Vicente; Multifunctional poly(glycolic acid-co-propylene fumarate) electrospun fibers reinforced with graphene oxide and hydroxyapatite nanorods. *Journal of Materials Chemistry B* **2017**, 5, 4084-4096, [10.1039/c7tb00497d](https://doi.org/10.1039/c7tb00497d).
60. Beiranvand, M.; Farhadi, S.; Mohammadi, A.; Graphene Oxide/Hydroxyapatite/Silver (rGO/HAP/Ag) nanocomposite: Synthesis, characterization, catalytic and antibacterial activity. *Int. J. Nano Dimens.* **2019**, 10, 180–194, .

Retrieved from <https://encyclopedia.pub/entry/history/show/8724>